

## EXAFS analysis of xanthine oxidase complexes with alloxanthine, violapterin, and 6-pteridylaldehyde

R. Hille, G. N. George, M. K. Eidsness, and S. P. Cramer

*Inorg. Chem.*, **1989**, 28 (21), 4018-4022 • DOI: 10.1021/ic00320a016

Downloaded from <http://pubs.acs.org> on November 16, 2008

### More About This Article

---

The permalink <http://dx.doi.org/10.1021/ic00320a016> provides access to:

- Links to articles and content related to this article
- Copyright permission to reproduce figures and/or text from this article



**Acknowledgment.** We are grateful to M. W. Perkovic for assistance with some of the calculations, to Professor H. B. Schlegel for providing us with access to the MODEL program, and to Dr. C. Creutz for providing us with pertinent information prior to publication. We are also grateful to the Chemistry Department at Brookhaven National Laboratory for allowing us to monitor a few reactions with their NMR spectrometer. The initial coordinates for the MM2 calculations were derived from those of the corresponding methyl-aquo complexes. These were initially set up by using The Ohio State University Chemistry Department's Image Center with a great deal of assistance from Dr. W.-K. Lin.

We are very appreciative of this assistance. C.L.S. gratefully acknowledges partial support through a Graduate and Professional Opportunities Scholarship from the Department of Education.

**Registry No.** Co(*ms*-(*N*)-Me<sub>6</sub>[14]dieneN<sub>4</sub>)Cl<sub>2</sub><sup>+</sup>, 55058-00-9; Co(*rac*-(*N*)-Me<sub>6</sub>[14]dieneN<sub>4</sub>)Cl<sub>2</sub><sup>+</sup>, 122742-53-4; [Sec-Cl]-Co(*rac*-(*N*)-Me<sub>6</sub>[14]dieneN<sub>4</sub>)(OH<sub>2</sub>)Cl<sub>2</sub><sup>+</sup>, 121701-57-3; [Pri-Cl]-Co(*rac*-(*N*)-Me<sub>6</sub>[14]dieneN<sub>4</sub>)(OH<sub>2</sub>)Cl<sub>2</sub><sup>+</sup>, 122742-54-5; Co(*ms*-(*N*)-Me<sub>6</sub>[14]dieneN<sub>4</sub>)(OH<sub>2</sub>)Cl<sub>2</sub><sup>+</sup>, 121701-57-3; NCS<sup>-</sup>, 302-04-5.

**Supplementary Material Available:** A table listing a typical set of MM2 parameters for metal-ligand interactions (2 pages). Ordering information is given on any current masthead page.

Contribution from the Department of Physiological Chemistry, College of Medicine, The Ohio State University, Columbus, Ohio 43210, Corporate Research Science Laboratories, Exxon Research and Engineering Company, Annandale, New Jersey 08801, Department of Chemistry, University of Georgia, Athens, Georgia 30602, and National Synchrotron Light Source, Brookhaven National Laboratory, Upton, New York 11973

## EXAFS Analysis of Xanthine Oxidase Complexes with Alloxanthine, Violapterin, and 6-Pteridylaldehyde<sup>⊥</sup>

R. Hille,<sup>†</sup> G. N. George,<sup>‡</sup> M. K. Eidsness,<sup>§</sup> and S. P. Cramer<sup>\*.||</sup>

Received September 9, 1988

The structure of the molybdenum site of xanthine oxidase in the complexes with alloxanthine, violapterin, and 6-pteridylaldehyde has been investigated by using X-ray absorption spectroscopy. The strongest component in the EXAFS spectrum is assigned to Mo-S bonds at  $2.38 \pm 0.03$ ,  $2.40 \pm 0.03$ , and  $2.46 \pm 0.03$  Å, respectively. In all cases, a second EXAFS component was identified as corresponding to a terminal oxo group with a bond length of 1.66-1.71 Å. A terminal sulfur ligand, with a Mo=S bond length of  $2.20 \pm 0.03$  Å, was observed for the oxidized 6-pteridylaldehyde complex. However, the presence of a short Mo=S bond ( $\leq 2.30$  Å) was ruled out for the alloxanthine and violapterin complexes. The EXAFS results are compared with previous proposals for the alloxanthine-xanthine oxidase complex.

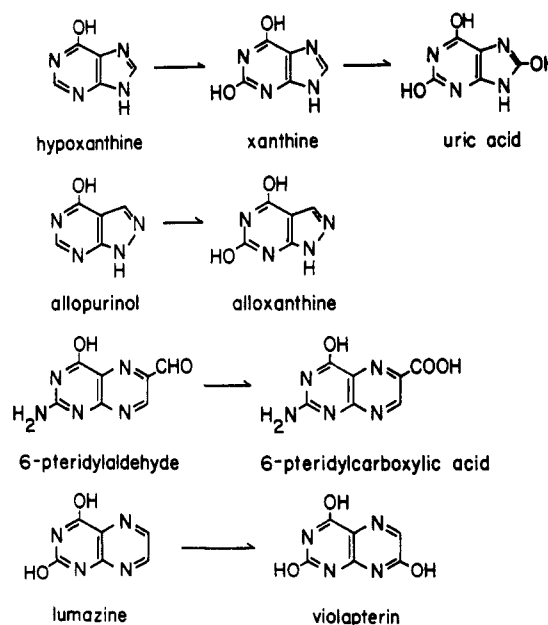
### Introduction

Xanthine oxidase (XO) is an enzyme containing molybdenum, FAD, and (2Fe-2S) clusters, which catalyzes the oxidations of hypoxanthine to xanthine and xanthine to uric acid, reactions that take place at the molybdenum center of the enzyme.<sup>1</sup> A variety of aromatic heterocycles form complexes at the molybdenum center that are of potential relevance to the catalytic cycle, as illustrated in Scheme I.

Alloxanthine (1*H*-pyrazolo[3,4-*d*]pyrimidine-4,6-diol) forms a tight complex with the Mo(IV) site of reduced xanthine oxidase.<sup>2</sup> This complex is of clinical importance because it is the inhibitory product of the reaction of xanthine oxidase with allopurinol (1*H*-pyrazolo[3,4-*d*]pyrimidin-4-ol) used in the treatment of hyperuricaemia.<sup>3</sup> The electron paramagnetic resonance (EPR) spectrum of the Mo(V)-alloxanthine complex with XO<sup>4-6</sup> is similar to the Very Rapid signal, which arises from a transient intermediate thought to be of catalytic significance<sup>7,8</sup> in the oxidation of xanthine and other substrates.<sup>8,9</sup> The similarity of the Mo(V) EPR signals suggests some degree of structural homology between the alloxanthine complex and the Very Rapid intermediate. Information about the alloxanthine complex is thus ultimately relevant to the catalytic mechanism of xanthine oxidase.

Violapterin (2,4,7-trihydroxypteridine) is the product of xanthine oxidase acting on the substrate lumazine (2,4-dihydroxypteridine) and forms a catalytically important complex with the reduced Mo(IV) enzyme.<sup>10</sup> This complex exhibits a long wavelength (650 nm) absorption band and is thought to correspond to a product complex (E<sub>red</sub>P) in the catalytic cycle. Davis et al. have labeled this a "charge-transfer" complex in which the molybdenum center of the enzyme is assigned as the donor and

**Scheme I.** Structures and Reactions of Xanthine Oxidase Substrates and Inhibitors



violapterin is assigned as the acceptor.<sup>10</sup> Pteridylaldehyde (2-amino-4-hydroxy-6-formylpteridine) forms a complex with a

<sup>†</sup> The Ohio State University.

<sup>‡</sup> Exxon Research and Engineering Co.

<sup>§</sup> University of Georgia.

<sup>\*</sup> Brookhaven National Laboratory.

<sup>||</sup> Abbreviations: FAD, flavin adenine dinucleotide; XO, xanthine oxidase; XAS, X-ray absorption spectroscopy; EXAFS, extended X-ray absorption fine structure.

(1) Hille, R.; Massey, V. *Molybdenum Enzymes*; Spiro, T. G., Ed.; John Wiley: New York, 1985; pp 443-518.

(2) Massey, V.; Komi, H.; Palmer, G.; Eliou, G. B. *J. Biol. Chem.* **1970**, *245*, 2837-2844.

(3) Wade, A., Ed. *Martindale: The Extra Pharmacopoeia*, 27th ed.; The Pharmaceutical Press: London, 1977; pp 371-372.

(4) Tanner, S. J. Ph.D. Thesis, University of Sussex, 1978.

(5) Williams, J. W.; Bray, R. C. *Biochem. J.* **1981**, *195*, 753-760.

(6) Hawkes, T. R.; George, G. N.; Bray, R. C. *Biochem. J.* **1984**, *218*, 961-968.

similar long-wavelength absorption band with xanthine oxidase in its oxidized Mo(VI) form.<sup>11</sup> This complex may be some sort of Michaelis complex ( $E_{ox}\text{-S}$ ), as pteridylaldehyde is in fact a slow substrate for xanthine oxidase, being slowly oxidized to the corresponding 6-carboxylate.

X-ray absorption spectroscopy (XAS) has proven a valuable probe of structure in xanthine oxidase as isolated<sup>12,13</sup> and complexed with arsenite.<sup>14</sup> In order to better understand the structure of the molybdenum site in the complexes of xanthine oxidase with alloxanthine, violapterin, and pteridylaldehyde, we have examined all three species by XAS and compared the spectra with those of model compounds.

### Experimental Section

**Materials.** Xanthine oxidase was prepared from unpasteurized milk by the method of Massey et al.<sup>9</sup> The folate affinity procedures described by Nishino et al.<sup>15</sup> were used both as a final step in the purification procedure and to separate the nonfunctional (desulfo) form of the enzyme from the functional form. Enzyme thus obtained was typically 95% active, estimated with respect to the theoretical activity of 100% active enzyme.<sup>16</sup> Samples for XAS were concentrated by vacuum dialysis against 0.1 M Bicine, pH 8.3, containing 0.1 mM EDTA to a concentration of approximately 1 mM. In the case of the alloxanthine complex, the sample was made 10 mM in alloxanthine, reduced with an excess of solid sodium dithionite, sealed in an EXAFS cell, and frozen on dry ice after a 15-min incubation. After the EXAFS spectrum was recorded, the sample was thawed under anaerobic conditions, an aliquot was diluted into nitrogen-equilibrated buffer, and its visible absorption spectrum was recorded to confirm that the sample had remained reduced in the X-ray beam. The diluted sample was subsequently reoxidized with a stream of air and its spectrum again recorded to confirm that alloxanthine had remained complexed to the enzyme.

The violapterin complex was prepared by essentially the same procedure as the alloxanthine complex, except that on dilution for determination of the sample integrity, the anaerobic buffer was also 2mM in violapterin. After the spectrum was recorded, the diluted sample was assayed and found to have lost no more than 10% of its original activity. For this sample, violapterin was prepared by enzymic action on lumazine, purchased from Aldrich and recrystallized as described by Davis et al.,<sup>10</sup> in 10 mM  $(\text{NH}_4)_2\text{CO}_3$ , pH 8.0, followed by lyophilization. The product was recrystallized three times from water prior to use.

The 6-pteridylaldehyde complex was prepared by making an aerobic sample of enzyme 10 mM in the heterocycle and freezing after a 2-min incubation. As with the violapterin complex, after acquisition of the EXAFS data, the sample was diluted and assayed and its spectrum recorded to confirm that the complex had remained intact. The 6-pteridylaldehyde used in these studies was the generous gift of Dr. Vincent Massey, Department of Biological Chemistry, The University of Michigan.

The model compounds  $\text{LMo}^{\text{VO}}(\text{SC}_6\text{H}_5)_2$ , where L is the anion of hydrotris(3,5-dimethylpyrazoyl)borate,<sup>17</sup>  $\text{LMo}^{\text{VO}}[\text{S}_2\text{CN}(n\text{-Bu})_2]$  and  $\text{LMo}^{\text{VS}}[\text{S}_2\text{CN}(n\text{-Bu})_2]$ , where  $[\text{S}_2\text{CN}(n\text{-Bu})_2]$  is the di-*n*-butyldithiocarbamate anion,<sup>18</sup> were prepared by literature procedures and kindly provided by Prof. John Enemark at the University of Arizona.

**Data Collection and Analysis.** The XAS spectra were measured at the Stanford Synchrotron Radiation Laboratory during 3-GeV dedicated operation on wiggler-beam lines IV-2 or VII-3 by using Si(2,2,0) monochromators. The ring current was generally 30–60 mA, yielding a flux on the order of  $10^9$  photons/s in the slitted 1 mm  $\times$  1 cm beam. For low-temperature operation samples were maintained at close to 4 K during data collection by using an Oxford Instruments CF204 cryostat.

- (7) Bray, R. C. *Adv. Enzymol. Relat. Areas Mol. Biol.* **1980**, *51*, 107–165.
- (8) Bray, R. C.; George, G. N. *Biochem. Soc. Trans.* **1985**, *13*, 560–567.
- (9) Massey, V.; Brumby, P. E.; Komai, H.; Palmer, G. *J. Biol. Chem.* **1969**, *244*, 1682–1691.
- (10) Davis, M. D.; Olson, J. S.; Palmer, G. *J. Biol. Chem.* **1982**, *257*, 14730–14737.
- (11) Hille, R.; Massey, V. *Pharmacol. Ther.* **1981**, *14*, 249–263.
- (12) Bordas, J.; Bray, R. C.; Garner, C. D.; Gutteridge, S.; Hasnain, S. S. *Biochem. J.* **1980**, *499*–508.
- (13) Cramer, S. P.; Wahl, R.; Rajagopalan, K. V. *J. Am. Chem. Soc.* **1981**, *103*, 7721–7727.
- (14) Cramer, S. P.; Hille, R. *J. Am. Chem. Soc.* **1985**, *107*, 8164–8169.
- (15) Nishino, T.; Nishino, T.; Tsushima, K. *FEBS Lett.* **1981**, *131*, 369–372.
- (16) Bray, R. C. *Enzymes* **1975**, *12*, 299–412.
- (17) Cleland, W. E., Jr.; Barnhart, K. M.; Yamanouchi, K.; Collison, D.; Mabbs, F. E.; Ortega, R. B.; Enemark, J. H. *Inorg. Chem.* **1987**, *26*, 1017–1025.
- (18) Young, C. G.; Roberts, S. A.; Ortega, R. B.; Enemark, J. H. *J. Am. Chem. Soc.* **1987**, *109*, 2938–2946.

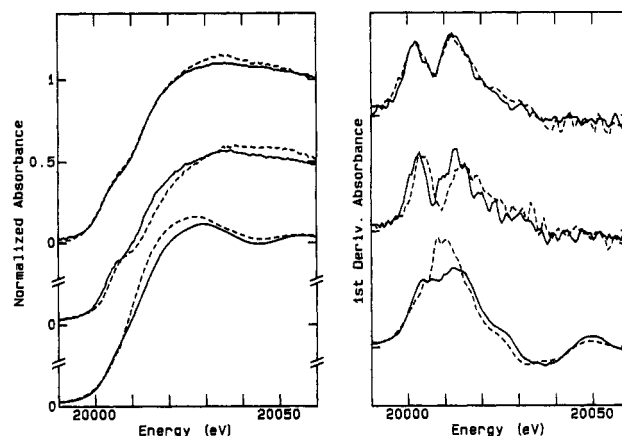


**Figure 1.** Mo K-edge (left) and derivative spectra (right): (top to bottom) alloxanthine-inhibited XO (—) vs dithionite-reduced XO (---);<sup>14</sup> violapterin-XO (—) vs pteridylaldehyde-XO (---);  $\text{LMoO}[\text{S}_2\text{CN}(n\text{-Bu})_2]$  (—) vs  $\text{LMoS}[\text{S}_2\text{CN}(n\text{-Bu})_2]$  (---). Spectra were normalized vs a cubic spline through the EXAFS at 20 125 eV.

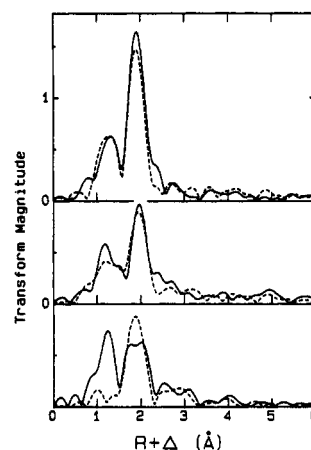


**Figure 2.** EXAFS Fourier transforms: (top to bottom) alloxanthine-inhibited XO (—) vs dithionite-reduced XO (---);<sup>14</sup> violapterin-XO (—) vs pteridylaldehyde-XO (---);  $\text{LMoO}[\text{S}_2\text{CN}(n\text{-Bu})_2]$  (—) vs  $\text{LMoS}[\text{S}_2\text{CN}(n\text{-Bu})_2]$  (---). Transform range:  $k = 4\text{--}14 \text{ \AA}^{-1}$ ;  $k^3$  weighting.

For the enzyme samples, fluorescence detection using zirconium filters and a slit assembly was employed.<sup>19</sup> The reported protein spectra represent the average of 8–12 20-min scans, with each detector operating at about 100 kHz, 5–25% of which was Mo fluorescence. During storage and shipping the enzyme samples were maintained at liquid-nitrogen temperature. The model compound data were recorded at 4 K ( $\text{LMo}^{\text{VE}}[\text{S}_2\text{CN}(n\text{-Bu})_2]$ ) or room temperature ( $\text{LMo}^{\text{VO}}(\text{SC}_6\text{H}_5)_2$ ) in transmission mode. All of the data collection used a three-ion-chamber geometry for a simultaneous Mo foil calibration, with the first inflection point defined as 20 003.9 eV.

The spectra were processed and interpreted by using previously described procedures.<sup>13,14,20,21</sup> For curve-fitting analysis, the spectra were smoothed by convolution with a  $0.1 \text{ \AA}^{-1}$  Gaussian function (fwhm). This improved the residual error function but did not significantly alter the optimized structural values.

### Results

**Edges.** The molybdenum K-edge region for alloxanthine-inhibited xanthine oxidase is compared with the spectrum of dithionite-reduced xanthine oxidase in Figure 1. A strong shoulder at about 20 003 eV is observed in both enzyme spectra. Theoretical calculations have assigned such features to transitions between the Mo 1s orbital and antibonding orbitals oriented along Mo=O or Mo=S bonds.<sup>22</sup> In Figure 1, spectra for the model compounds

- (19) Cramer, S. P.; Scott, R. A. *Rev. Sci. Instrum.* **1981**, *52*, 395–399.
- (20) Cramer, S. P. *EXAFS for Inorganic Systems*; Garner, C. D., Hasnain, S. S., Eds.; Daresbury Lab: Daresbury, England, 1981; pp 47–50.
- (21) Cramer, S. P.; Solomonson, L. P.; Adams, M. W. W.; Mortenson, L. E. *J. Am. Chem. Soc.* **1984**, *106*, 1467–1471.
- (22) Kutzler, F. W.; Scott, R. A.; Berg, J. M.; Hodgson, K. O.; Doniach, S.; Cramer, S. P.; Chang, C. H. *J. Am. Chem. Soc.* **1980**, *103*, 6083–6088.

Table I. Xanthine Oxidase Complex and Model Compound Curve-Fitting Results

sample	Mo-SR			Mo=O(S)			Mo-X			residual <sup>f</sup>	
	N <sup>a</sup>	R <sup>b</sup> , Å	10 <sup>3</sup> σ <sup>2</sup> , Å <sup>2</sup>	N	R, Å	10 <sup>3</sup> σ <sup>2</sup> , Å <sup>2</sup>	X <sup>d</sup>	N	R, Å		10 <sup>3</sup> σ <sup>2</sup> , Å <sup>2</sup>
LMOs <sub>2</sub> CN( <i>n</i> -Bu) <sub>2</sub> diffraction <sup>f</sup>	2	2.443	317	1	1.662	102	O, N	2	2.162	520	0.548
	2	2.442		1	1.669		N	2	2.180		
LMOSS <sub>2</sub> CN( <i>n</i> -Bu) <sub>2</sub> diffraction <sup>f</sup>	2	2.436	452	1	2.117	139	O, N	2	2.168	729	0.682
	2	2.434		1	2.129		N	2	2.181		
LMO(SC <sub>6</sub> H <sub>5</sub> ) <sub>2</sub> diffraction <sup>g</sup> dithionite reduced xanthine oxidase	2	2.357	256	1	1.669	23	O, N	2	2.148	330	0.662
	2	2.382		1	1.676		N	2	2.185		
	2	2.378	45								2.675
alloxanthine-inhibited xanthine oxidase	3	2.381	219								2.305
	4	2.382	367								2.369
	3	2.381	208	1	1.672	153					0.887
	3	2.380	451	1	1.664	174	O, N	1	2.243	-202	0.552
	3	2.365	540	1	1.665	178	O, N	2	2.253	-1	0.586
	2	2.383	-21								2.628
	3	2.384	141								2.083
	4	2.385	276								2.138
	3	2.385	129	1	1.679	148					0.798
	3	2.381	220	1	1.676	183	O, N	1	2.255	60	0.656
violapterin xanthine oxidase	3	2.380	155	1	1.677	176	O, N	2	2.273	811	0.656
	2	2.384	6	1	1.679	158	O, N	2	2.204	364	0.660
	2	2.400	159								2.031
	3	2.399	380								2.273
	2	2.400	149	1	1.662	290					1.109
pteridylaldehyde xanthine oxidase	2	2.400	122	1	1.665	262	O, N	1	2.079	305	0.934
	3	2.400	357	1	1.661	271	O, N	1	2.072	139	1.199
	2	2.447	231								3.047
	3	2.481	515								3.537
	2	2.473	222	1	1.714	340					2.276
2	2.456	395	1	1.710	251	S, Cl	1	2.195	40	0.634	

<sup>a</sup> Coordination number; fixed at reported integral values during refinement. <sup>b</sup> Interatomic distance; systematic error ca. 0.02 Å. <sup>c</sup> Mean-square deviation of *R*; negative values arise if postulated *N* is low or if amplitude function is inaccurate. <sup>d</sup> Ligand type; same functions used for Mo-N and Mo-O interactions. <sup>e</sup> Fit residual; defined as  $(\sum(\chi_{\text{exp}} - \chi_{\text{calc}})^2/k^6)/N$ . <sup>f</sup> Reference 16. <sup>g</sup> Reference 17 (long Mo-N not included in analysis).

LMO[S<sub>2</sub>CN(*n*-Bu)<sub>2</sub>] and LMO[S<sub>2</sub>CN(*n*-Bu)<sub>2</sub>] are also shown. The bound-state transition feature is weaker in the oxo-molybdenum model compound and almost invisible in the terminal sulfur analogue.

Figure 1 also shows the Mo K absorption edge spectra of the violapterin and pteridylaldehyde xanthine oxidase complexes. Both spectra exhibit shoulders on the edge similar to the cases described above. The violapterin spectrum is shifted to lower energy than the pteridylaldehyde spectrum. This is in accord with violapterin forming a complex with reduced xanthine oxidase and pteridylaldehyde forming a complex with the oxidized enzyme.

**EXAFS.** The Fourier transforms of the Mo EXAFS data for the various complexes of xanthine oxidase and relevant model compounds are compared in Figure 2. In all cases, the strongest peak is consistent with a long Mo-S interaction. For the enzyme spectra, the EXAFS analysis alone cannot exclude an overlapping Mo-Cl interaction in this region. Apart from the spectrum of the Mo=S model compound, all spectra also show a peak at  $R + \Delta \cong 1.2$  Å, attributable to a Mo=O interaction at a true distance of  $\sim 1.7$  Å. However, the model compound spectra show that other Mo-ligand interactions known to be present, such as Mo-N interactions, are not always resolved in the Fourier transform. For a more quantitative interpretation of the spectra, curve-fitting analysis was employed.

The spectra were analyzed quantitatively by curve-fitting of the *k*-space data using previously described empirical phase shift and amplitude functions.<sup>13,20,21</sup> The procedure began by generating the best possible fit with a single shell or sulfur ligands assigned to the main Fourier transform peak. In all of the xanthine oxidase data, this corresponds to a set of two to three sulfurs at approximately 2.4 Å. A "search profile" was then generated to help identify the nature of the second largest transform peak. The search profiles (Figure 3) show the quality of fit as a function of the distance at which a component is added, while keeping other structural parameters constant. The "base-line" values (no added component) for these curves are the corresponding lowest residual single-shell Mo-S fits in Table I.

For alloxanthine-inhibited xanthine oxidase, the fit was dramatically improved by using a Mo=O interaction at 1.68 Å, as

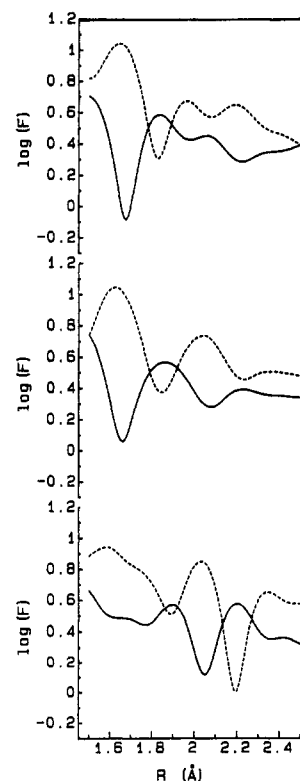
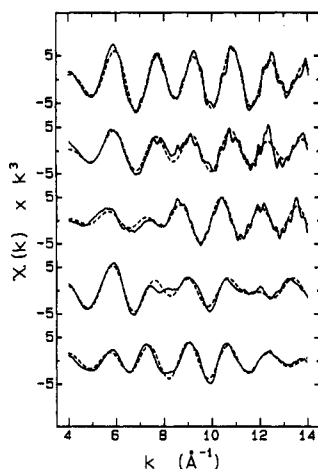


Figure 3. Search profiles for adding one Mo-O (—) or one Mo-S' (---) after fitting long Mo-SR interaction: (top to bottom) alloxanthine-inhibited XO; violapterin-XO; pteridylaldehyde-XO.

illustrated in Figure 3. In contrast, inclusion of a short Mo=S interaction did not make a significant improvement in the fit. After the two-shell fit was optimized with these Mo-S and Mo=O components, a second search profile was generated for minor Mo-X interactions, where X could be (S, Cl) or (N, O). One or two additional nitrogens and/or oxygens could be included



**Figure 4.** Smoothed experimental data (—) and lowest residual fit (---): (top to bottom) alloxanthine-inhibited XO; violapterin-XO; pteridylaldehyde-XO;  $\text{LMoO}[\text{S}_2\text{CN}(n\text{-Bu})_2]$ ;  $\text{LMoS}[\text{S}_2\text{CN}(n\text{-Bu})_2]$ .

at about 2.25 Å with some modest improvement in the fit. Figure 3 also shows the corresponding initial search profiles for the XO violapterin and pteridylaldehyde complexes, respectively.

The final fits for the enzyme and model compound spectra are shown in Figure 4, and the results are summarized in Table I. The model compound EXAFS analysis generally agreed with crystallographic distances to 0.02 Å. This is the average accuracy for multishell curve-fitting analysis. Distances are quoted to 0.001 Å in Table I solely to avoid generating additional round-off errors.

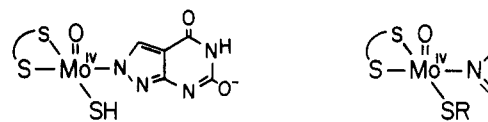
All enzyme complexes were found to contain short  $\text{Mo}=\text{O}$  as well as long  $\text{Mo}-\text{S}$  interactions. The oxidized pteridylaldehyde-enzyme complex has a primary  $\text{Mo}-\text{S}$  bond length of 2.46 Å, 0.06 Å longer than the  $\text{Mo}-\text{S}$  distance in the reduced violapterin-enzyme complex. This is consistent with previous EXAFS results with oxidized XO, which generally find a relatively long  $\text{Mo}$ -“thiolate” bond length. An important result of the curve-fitting analysis is that a terminal  $\text{Mo}=\text{S}$  interaction at 2.20 Å was observed for the oxidized pteridylaldehyde complex, while such a short  $\text{Mo}=\text{S}$  interaction was not seen for the reduced violapterin complex.

### Discussion

Because the EXAFS results pertain to the  $\text{Mo(IV)}$  state of the alloxanthine complex, whereas the EPR data reflect the  $\text{Mo(V)}$  alloxanthine complex, a direct comparison of spectroscopic findings is not currently possible. Nevertheless, the EXAFS results can address some of the proposed  $\text{Mo(IV)}$  species, and conclusions about the  $\text{Mo(V)}$  species can be reached with some inference. In any case, it must be kept in mind that  $\text{Mo(IV)}$  is the relevant oxidation state with respect to the enzyme-alloxanthine complex as it is generally prepared.<sup>2</sup>

On the basis of the present EXAFS analysis, the molybdenum site of the alloxanthine-complexed XO complex appears to be structurally very similar to the dithionite-reduced enzyme.<sup>13,14</sup> In both cases, the enzyme is in the reduced  $\text{Mo(IV)}$  state and the ligands include two to three thiolate-like sulfurs and a single oxo group. It is worth noting that assignment as thiolate-like sulfur is based on chemical analogy with known complexes with similar bond lengths; EXAFS alone cannot distinguish thiolate from thioether or other forms of sulfur or even from chloride for that matter. All of the EXAFS data on reduced forms of XO, including violapterin-XO, alloxanthine-XO, complexes with arsenite or 8-bromoxanthine,<sup>14</sup> and even rapidly frozen intermediates<sup>23</sup>

**Chart I.** Structures for the Alloxanthine Complex Consistent with EPR and EXAFS Results



suggest that the terminal oxo group is not protonated upon reduction from  $\text{Mo(VI)}$  to  $\text{Mo(IV)}$ . Rather, it appears that a better formulation for the terminal ligation in the fully reduced enzyme is  $\text{O}=\text{Mo}-\text{SH}$  or  $\text{O}=\text{Mo}-\text{SR}$ , where R is a group that binds to and lengthens the original  $\text{Mo}=\text{S}$  species.

Apart from the EXAFS results, a valid proposal for the structure of the inhibitory complex must take into account the following additional information. First, the  $\text{Mo(IV)}$  alloxanthine complex is kinetically reasonably stable toward reoxidation by molecular oxygen. Rather specific redox conditions are required to obtain the EPR-detectable  $\text{Mo(V)}$ .<sup>6</sup> Second, the reduced  $\text{Mo(IV)}$ -containing enzyme is required for complex formation.<sup>2</sup> Third, alloxanthine forms a tight complex, whereas allopurinol does not.<sup>2</sup> Finally, the EPR signal obtained on partial oxidation of the enzyme-alloxanthine complex does not exhibit any detectable hyperfine coupling from exchangeable protons, but shows resolved <sup>14</sup>N hyperfine coupling.<sup>6</sup> The latter coupling may originate from a coordinated nitrogen from the alloxanthine molecule,<sup>6</sup> although other sources for the nitrogen ligand, such as the  $\text{Mo}$ -co-pterin moiety, have not yet been ruled out. In light of these facts, two structures consistent with the EXAFS are proposed in Chart I.

Hawkes et al. have discussed the strong resemblance between the EPR spectrum of the Very Rapid species, which is observed as a transient in the oxidation of xanthine, and the signal from the  $\text{Mo(V)}$  form of the alloxanthine complex.<sup>6</sup> Apart from close correspondence in g values, both spectra exhibit very similar <sup>33</sup>S hyperfine couplings upon enrichment with <sup>33</sup>S, with comparable angular relationships between the g and A tensors. However, whereas in the Very Rapid signal strong isotropic coupling to an <sup>17</sup>O nucleus can be observed upon enrichment, no such coupling is present for the alloxanthine signal, but coupling to a single nitrogen atom is seen.<sup>6</sup> On the basis of these and other findings, Hawkes et al. have proposed a structural parallel between the xanthine Very Rapid species and the alloxanthine species. Our results with alloxanthine-complexed enzyme indicate that if this structural parallel is correct, the  $\text{Mo(IV)}$  redox partner of the  $\text{Mo(V)}$  species giving rise to the Very Rapid EPR signal also has an intact  $\text{Mo}=\text{O}$  group, a conclusion supported by preliminary rapid-freeze EXAFS results.<sup>23</sup> One explanation for the lack of exchangeable proton coupling in the EPR of species a in Chart I would be deprotonation upon oxidation from  $\text{Mo(IV)}$  to  $\text{Mo(V)}$ . An alternate explanation, shown as species b in Chart I, is that the sulfido interacts with some group R to cause  $\text{Mo}-\text{S}$  bond lengthening in the  $\text{Mo(IV)}$  species.

Since the EXAFS oscillations are so well accounted for by  $\text{Mo}=\text{O}$  and  $\text{Mo}-\text{SR}$  components, it is difficult to say much about the remaining  $\text{Mo}-\text{O,N}$  coordination. The addition of another  $\text{Mo}-\text{O,N}$  component generally reduced the residual by 15–20%, and the distances obtained are chemically reasonable. However, the fits are not sensitive to the postulated  $\text{Mo}-\text{O,N}$  coordination number, one or two nitrogens or oxygens in the vicinity of 2.1–2.2 Å give equally good fits. Clearly, this is a case where EXAFS (which is quite sensitive to sulfur or oxo coordination) and EPR (which can observe hyperfine interactions from weakly bound oxygens or nitrogens) have complementary capabilities.

With regard to the EXAFS of the violapterin and pteridylaldehyde xanthine oxidase complexes, the data clearly indicate the presence of oxo and thiolate-like ligands coordinated to molybdenum in both the reduced and oxidized forms of the enzyme. These complexes differ from one another in that the oxidized enzyme also shows  $\text{Mo}=\text{S}$  coordination. In the reduced enzyme, this sulfido sulfur is no longer resolved, presumably because it is protonated, with an  $\text{Mo}-\text{SH}$  distance similar to the  $\text{Mo}-\text{SR}$

(23) George, G. N.; Bray, R. C.; Cramer, S. P. *Biochem. Soc. Trans.* **1986**, *14*, 651–652.

(24) Alternatively, one could hypothesize a  $\text{O}=\text{Mo}(\text{SH})(\text{OH})$  structure for the reduced enzyme, but this leads to difficulties in the higher oxidation states. Successive deprotonations upon oxidation from  $\text{Mo(IV)}$  to  $\text{Mo(VI)}$  would be expected to yield a structure with three short terminal ligands:  $\text{Mo(O)}_2(\text{S})$ . An  $\text{Mo(O)}(\text{S})$  species is observed in the current and past data.<sup>13,14</sup>

values. Also, the pteridylaldehyde Mo—S and Mo=O bonds distances are longer by about 0.06 and 0.04 Å, respectively, from those in the violapterin complex.

All the Mo—ligand distances in the 6-pteridylaldehyde complex are slightly longer than in the free oxidized enzyme.<sup>14</sup> The effect is most pronounced for the Mo=S bond, which lengthens by some 0.05 Å on binding of 6-pteridylaldehyde. Such changes, which are on the threshold of significance for an EXAFS measurement, might occur through an increase in the molybdenum coordination number or through a weak association of pteridylaldehyde with the terminal Mo ligands.

The presence of a long-wavelength absorption band in the electronic spectra of the violapterin complex has been interpreted as involving a charge-transfer complex between the molybdenum center and heterocycle.<sup>10</sup> However, by X-ray absorption, the complex of violapterin with reduced enzyme is nearly indistinguishable from the free reduced enzyme. Also, a similar electronic absorption band is observed for the pteridylaldehyde complex.<sup>11</sup> An alternative explanation is that the absorption bands represent charge-transfer complexes between the pterin of the molybdenum cofactor<sup>25</sup> and the bound heterocycle. Such an assignment would be consistent with the EXAFS results, which show rather small changes in Mo site radial distances. However, the loss of this absorption band upon cyanolytic removal of the terminal sulfur remains unexplained.

### Conclusions

Along with thiolate-like sulfurs presumably donated by the molybdenum cofactor, X-ray absorption spectroscopy clearly reveals a terminal Mo=O bond in the xanthine oxidase alloxanthine complex and, equally important, shows the absence of a short Mo=S bond in the Mo(IV) complex. The EPR spectrum of the corresponding Mo(V) complex exhibits an unusually large

<sup>33</sup>S hyperfine coupling and a lack of proton hyperfine coupling, which have been taken to indicate the presence of Mo=S in the signal-giving species. These data can be reconciled by postulating deprotonation of Mo<sup>IV</sup>—SH, upon oxidation, to Mo<sup>V</sup>=S. Recent EPR spectroscopic evidence supports a Mo(O)(S) structure for the Mo(V) Very Rapid species.<sup>26</sup> Less plausible alternatives invoke an unusual geometry for a Mo<sup>V</sup>—SH complex that would minimize proton hyperfine coupling or a covalent interaction for the Mo(IV) sulfido species to lengthen the terminal Mo=S bond.

The current results show that a Mo=O group is present at many points in the catalytic cycle of xanthine oxidase, being present in E<sub>ox</sub>·S (the 6-pteridylaldehyde complex), at least one intermediate encountered in the course of hydroxylation (the Very Rapid species, by analogy with the alloxanthine complex), and finally E<sub>red</sub>·P (the violapterin complex). This observation must be reconciled with recent evidence interpreted as indicating incorporation of oxygen from the Mo=O group into the product hydroxyl group in the course of catalysis.<sup>27</sup> We cannot exclude the involvement of a transient deoxy species in the catalytic cycle, on a time scale that is short compared to those of steady-state or rapid-freezing experiments. Detailed understanding of the catalytic mechanism of xanthine oxidase remains an elusive goal.

**Acknowledgment.** The spectra were recorded at the Stanford Synchrotron Radiation Laboratory, which is funded by the Department of Energy, Office of Basic Energy Sciences, and the National Institutes of Health, Biotechnology Resource Program, Division of Research Resources. This work was supported in part by Grant DMB-8521645 from the National Science Foundation (R.H.).

**Registry No.** Mo, 7439-98-7; O<sub>2</sub>, 7782-44-7; N<sub>2</sub>, 7727-37-9; LMo<sup>V</sup>-O(SC<sub>6</sub>H<sub>5</sub>)<sub>2</sub>, 105810-18-2; LMo<sup>IV</sup>O[S<sub>2</sub>CN(*n*-Bu)<sub>2</sub>], 107441-39-4; LMo<sup>IV</sup>S[S<sub>2</sub>CN(*n*-Bu)<sub>2</sub>], 107441-43-0.

(25) Cramer, S. P.; Stiefel, E. I. *Molybdenum Enzymes*; Spiro, T. G., Ed.; John Wiley: New York, 1985; pp 411-441.

(26) George, G. N.; Bray, R. C. *Biochemistry* **1988**, *27*, 3603-3609.

(27) Hille, R.; Sprecher, H. *J. Biol. Chem.* **1987**, *262*, 10914-10917.

Contribution from the Department of Chemistry,  
University of Kentucky, Lexington, Kentucky 40506-0055

## Triazaboles and Related Triazole Derivatives of Boron<sup>1</sup>

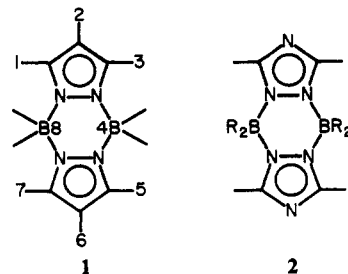
K. Niedenzu\* and K. R. Woodrum

Received April 5, 1989

The reaction of trimethylamine-borane, Me<sub>3</sub>N·BH<sub>3</sub>, with 1,2,4-triazole (=Hst) results in the formation of an oligomer mixture of the composition [H<sub>2</sub>B(st)]<sub>n</sub>; species with *n* up to 6 could be identified by mass spectrometry. Dimeric species = *sym*-triazaboles, R<sub>2</sub>B(μ-st)<sub>2</sub>BR<sub>2</sub> (**2**, R = hydrocarbon group), can be obtained in low yield from the condensation of R<sub>3</sub>B with Hst, from the interaction of halodiorganylboranes, R<sub>2</sub>BX (X = Cl, Br), with *N*-(trimethylsilyl)-1,2,4-triazole, Me<sub>3</sub>Si(st), and also by a transamination of a (dimethylamino)diorganylborane, Me<sub>2</sub>NBR<sub>2</sub>, with Hst. However, the major products are generally oligomeric materials [R<sub>2</sub>B(st)]<sub>n</sub>. The interaction of 3-amino-1,2,4-triazole (=Hat) with excess of R<sub>3</sub>B ultimately gives a reasonable yield of a mixture of two isomeric triazaboles of type **2** with the amino groups in either the 1,5- or 1,7-positions, whereas transamination of Me<sub>2</sub>NBR<sub>2</sub> with Hat preferentially gives the 1,5-diamino isomer but in low yield. Several boron derivatives of 1,2,3-triazoles have been isolated and characterized; these include tetrameric species (derived from 1,2,3-triazole = Hut or benzotriazole = Hbt) with a cyclic structure (**6**) resembling that of porphine, but also oligomeric materials [R<sub>2</sub>B(ut)]<sub>n</sub> and [R<sub>2</sub>B(bt)]<sub>n</sub>.

### Introduction

Although almost 100 different B- and/or C-substituted pyrazaboles (**1**), the neutral dimers of 1-pyrazolylboranes, are known, corresponding boron derivatives of triazoles, i.e., species where two four-coordinate boron atoms are linked by two triazolyl groups, have not yet been explored. Only one such compound, 4,4,8,8-tetraethyl-*sym*-triazabole (**2**, R = C<sub>2</sub>H<sub>5</sub>), has been described. This latter compound was obtained in moderate yield by the condensation reaction of Et<sub>3</sub>B with 1,2,4-triazole.<sup>3</sup> While the present



(1) Boron-Nitrogen Compounds. 121. Part 120: Mariategui, J. F.; Niedenzu, K. *J. Organomet. Chem.* **1989**, *369*, 137-145.

(2) Niedenzu, K.; Trofimenko, S. *Top. Curr. Chem.* **1986**, *131*, 1-37.

(3) Trofimenko, S. *J. Am. Chem. Soc.* **1967**, *89*, 3165-3170.

work was in progress, the interaction of 3-amino-1,2,4-triazole with an excess of trialkylboranes was reported to give reasonable yields of isomeric *sym*-triazaboles with NH<sub>2</sub> groups in either the 1,5- or 1,7-positions of **2** (R = C<sub>3</sub>H<sub>7</sub>, C<sub>4</sub>H<sub>9</sub>).<sup>4</sup>